

Search for the Blazhko effect in field RR Lyrae stars using LINEAR and ZTF light curves

Ema Donev¹ and Željko Ivezić²

¹ XV. Gymnasium (MIOC), Jordanovac 8, 10000, Zagreb, Croatia, e-mail: emadonev@icloud.com

² Department of Astronomy and the DiRAC Institute, University of Washington, 3910 15th Avenue NE, Seattle, WA, USA e-mail: ivezic@uw.edu

October 2024

ABSTRACT

We analyzed the incidence and properties of RR Lyrae stars that show evidence for amplitude and phase modulation (the so-called Blazhko Effect) in a sample of $\sim 3,000$ stars with LINEAR and ZTF light curve data. A preliminary subsample of about ~ 240 stars was algorithmically pre-selected using various data quality and light curve statistics, and then 139 stars were confirmed visually as displaying the Blazhko effect. This sample places a lower limit of 5% for the incidence of the Blazhko Effect in field RR Lyrae stars. Although close to 8,000 Blazhko stars were discovered or confirmed in the Galactic bulge and LMC/SMC by the OGLE-III survey, only about 200 stars have been reported in all field RR Lyrae stars studies to date; the sample presented here nearly doubles the number of field RR Lyrae stars displaying the Blazhko effect. With time-resolved photometry expected from LSST, a similar analysis will be performed for RR Lyrae stars in the southern sky and we anticipate a higher fraction of discovered Blazhko stars due to better sampling and superior photometric quality.

Key words. Variable stars — RR Lyrae stars — Blazhko Effect

1. Introduction

RR Lyrae stars are pulsating variable stars with periods in the range of 3–30 hours and large amplitudes that increase towards blue optical bands (e.g., in the SDSS g band from 0.2 mag to 1.5 mag; Sesar et al. 2010). For comprehensive reviews of RR Lyrae stars, we refer the reader to Smith (1995) and Catelan (2009).

RR Lyrae stars often exhibit amplitude and phase modulation, or the so-called Blazhko effect¹ (hereafter, “Blazhko stars”). For examples of well-sampled observed light curves showing the Blazhko effect, see, e.g., Kepler data shown in Figures 1 and 2 from Benkő et al. (2010). The Blazhko effect has been known for a long time (Blažko 1907), but its detailed observational properties and theoretical explanation of its causes remain elusive (Kolenberg 2008; Kovács 2009; Szabó 2014). Various proposed models for the Blazhko effect, and principal reasons why they fail to explain observations, are summarized in Kovacs (2016).

A part of the reason for the incomplete observational description of the Blazhko effect is difficulties in discovering a large number of Blazhko stars due to temporal baselines that are too short and insufficient number of observations per object (Kovacs 2016; Hernitschek & Stassun 2022). With the advent of modern sky surveys, several studies reported large increases in the number of known Blazhko stars, starting with a sample of about 700 Blazhko stars discovered by the MACHO survey towards the LMC (Alcock et al. 2003) and about 500 Blazhko stars discovered by the OGLE-II survey towards the Galactic bulge (Mizerski 2003). Most recently, about 4,000 Blazhko stars were discovered in the LMC and SMC (Soszyński et al. 2009, 2010),

and an additional $\sim 3,500$ stars were discovered in the Galactic bulge (Soszyński et al. 2011; Prudil & Skarka 2017), both by the OGLE-III survey. Nevertheless, discovering the Blazhko effect in field RR Lyrae stars that are spread over the entire sky remains a much harder problem: only about 200 Blazhko stars in total from all the studies of field RR Lyrae stars have been reported so far (see Table 1 in Kovacs 2016).

Here, we report the results of a search for the Blazhko effect in a sample of $\sim 3,000$ field RR Lyrae stars with LINEAR and ZTF light curve data. A preliminary subsample of about ~ 240 stars was selected using various light curve statistics, and then ~ 140 stars were confirmed visually as displaying the Blazhko effect. This new sample greatly increases the number of known field RR Lyrae stars that exhibit the Blazhko effect. In §2 and §3 we describe our datasets and analysis methodology, and in §4 we present our analysis results. Our main results are summarized and discussed in §5.

2. Data Description and Period Estimation

Analysis of field RR Lyrae stars requires a sensitive time-domain photometric survey over a large sky area. For our starting sample, we used $\sim 3,000$ field RR Lyrae stars with light curves obtained by the LINEAR asteroid survey. In order to study long-term changes in light curves, we also utilized light curves obtained by the ZTF survey which monitored the sky ~ 15 years after LINEAR. The combination of LINEAR and ZTF provided a unique opportunity to systematically search for the Blazhko effect in a large number of field RR Lyrae stars.

¹ The Blazhko effect was discovered by Lidiya Petrovna Tseraskaya and first reported by Sergey Blazhko.

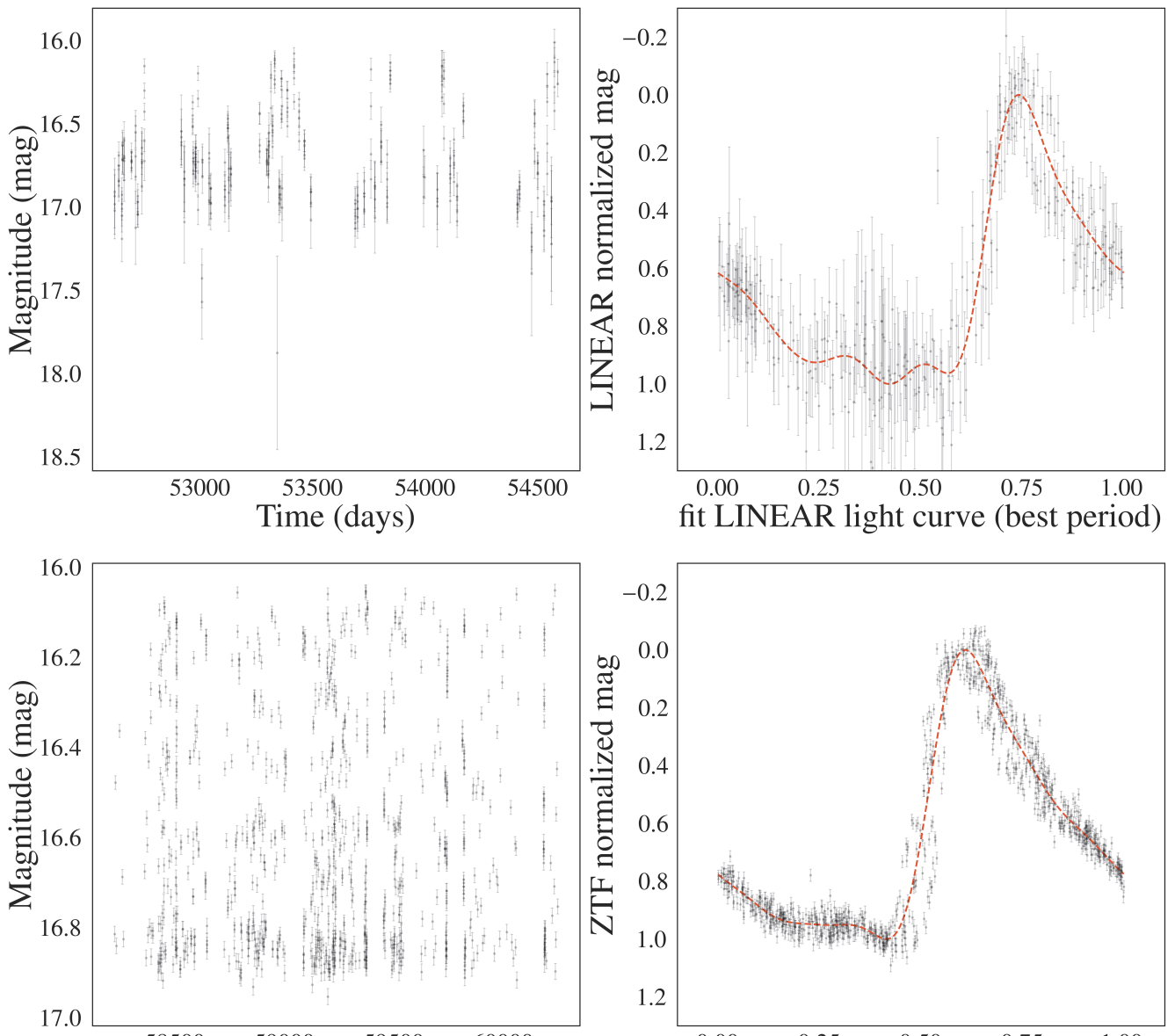


Fig. 1. An example of a Blazhko star (LINEARid = 1212611) with LINEAR (top row) and ZTF (bottom row) light curves (left panels, data points with “error bars”), phased light curves (norm. mag.) to the 0–1 range (right panels, data points with “error bars”), the best-fit model shown by dashed lines. The best-fit period is determined for each dataset separately using 3 Fourier terms. The models shown in the right panels are evaluated with 6 Fourier terms.

57 We first describe each dataset in more detail, and then introduce our analysis methods. All our analysis code, written in
 58 Python, is available on GitHub².
 59

60 2.1. LINEAR Dataset

61 The properties of the LINEAR asteroid survey and its photometric re-calibration based on SDSS data are discussed in Sesar
 62 et al. (2011). Briefly, the LINEAR survey covered about 10,000
 63 deg² of the northern sky in white light (no filters were used, see
 64 Figure 1 in Sesar et al. 2011), with photometric errors ranging
 65 from ~0.03 mag at an equivalent SDSS magnitude of $r = 15$ to
 66 0.20 mag at $r \sim 18$. Light curves used in this work include, on
 67 average, 270 data points collected between December 2002 and
 68 September 2008.
 69

70 A sample of 7,010 periodic variable stars with $r < 17$ discovered
 71 in LINEAR data were robustly classified by Palaversa et al.
 72 (2013), including about ~3,000 field RR Lyrae stars of both ab
 73 and c type, detected to distances of about 30 kpc (Sesar et al.
 74 2013). The sample used in this work contains 2196 ab-type and
 75 745 c-type RR Lyrae, selected using classification labels and the
 76 *gi* color index from Palaversa et al. (2013). The LINEAR light
 77 curves, augmented with IDs, equatorial coordinates, and other
 78 data, were accessed using the astroML Python module³ (VanderPlas
 79 et al. 2012).

80 2.2. ZTF Dataset

81 The Zwicky Transient Factory (ZTF) is an optical time-domain
 82 survey that uses the Palomar 48-inch Schmidt telescope and a

² https://github.com/emadonev/var_stars

³ For an example of light curves, see https://www.astroml.org/book_figures/chapter10/fig_LINEAR_LS.html

83 camera with 47 deg² field of view (Bellm et al. 2019). The
 84 dataset analyzed here was obtained with SDSS-like *g*, *r*, and *i*
 85 band filters. Light curves for objects in common with the LIN-
 86 EAR RR Lyrae sample typically have smaller random photomet-
 87 ric errors than LINEAR light curves because ZTF data are deeper
 88 (compared to LINEAR, ZTF data have about 2-3 magnitudes
 89 fainter 5 σ depth). ZTF data used in this work were collected be-
 90 tween February 2018 and December 2023, on average about 15
 91 years after obtaining LINEAR data.

92 The ZTF dataset for this project was created by selecting
 93 ZTF IDs with matching equatorial coordinates to a correspond-
 94 ing LINEAR ID of an RR Lyrae star. This process used the
 95 *ztfquery* function, which searched the coordinates in the ZTF
 96 database within 3 arcsec from the LINEAR position. The result-
 97 ing sample consisted of 2857 RR Lyrae stars with both LINEAR
 98 and ZTF data. The fractions of RRab and RRc type RR Lyrae in
 99 this sample, 71% RRab and 29% RRc type, are consistent with
 100 results from other surveys (e.g., Sesar et al. 2010).

101 2.3. Period Estimation

102 The first step of our analysis is estimating best-fit periods, sepa-
 103 rately for LINEAR and ZTF datasets. We used the Lomb-Scargle
 104 method (Vanderplas 2015) as implemented in *astropy* (Astropy
 105 Collaboration et al. 2018). The period estimation used 3 Fourier
 106 components and a two-step process: an initial best-fit frequency
 107 was determined using the *autopower* frequency grid option and
 108 then the power spectrum was recomputed around the initial fre-
 109 quency using an order of magnitude smaller frequency step. In
 110 case of ZTF, we estimated period separately for each available
 111 passband and adopted their mean value. Once the best-fit period
 112 was determined, a best-fit model for the phased light curve was
 113 computed using 6 Fourier components. Fig 1 shows an exam-
 114 ple of a star with LINEAR and ZTF light curves, phased light
 115 curves, and their best-fit models.

116 We found excellent agreement between the best-fit periods
 117 estimated separately from LINEAR and ZTF light curves. The
 118 median of their ratio is unity within 2×10^{-6} and the robust stan-
 119 dard deviation of their ratio is 2×10^{-5} . With a median sample
 120 period of 0.56 days, the implied scatter of period difference is
 121 about 1.0 sec.

122 Given on average about 15 years between LINEAR and ZTF
 123 data sets, and a typical period of 0.56 days, this time difference
 124 corresponds to about 10,000 oscillations. With a fractional pe-
 125 riod uncertainty of 2×10^{-5} , LINEAR data can predict the phase
 126 of ZTF light curve with an uncertainty of 0.2. Therefore, for a
 127 robust detection of light curve phase modulation, each data set
 128 must be analyzed separately. On the other hand, amplitude mod-
 129 ulation can be detected on time scales as long as 15 years, as
 130 discussed in the following section.

131 3. Analysis Methodology: Searching for the Blazhko 132 Effect

133 Given the two sets of light curves from LINEAR and ZTF, we
 134 searched for amplitude and phase modulation, either during the
 135 5-6 years of data taking by each survey, or during the average
 136 span of 15 years between the two surveys. Starting with a sam-
 137 ple of 2857 RR Lyrae stars, we pre-selected a smaller sample
 138 that was inspected visually (see below for details). We also re-
 139 quired at least 250 LINEAR data points and 40 ZTF data points
 140 (per band) in analyzed light curves. We used two pre-selection
 141 methods that are sensitive to different types of light curve mod-

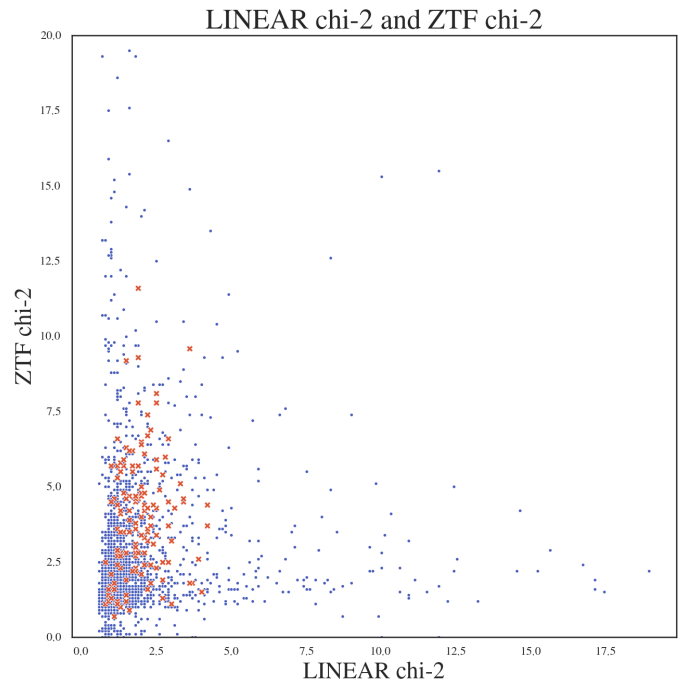


Fig. 2. A selection diagram constructed with the two sets of robust χ^2_{dof} values, for LINEAR and ZTF data sets, where blue symbols represents all RR Lyrae stars and the red symbols are the final sample of Blazhko stars. The horizontal and vertical dashed lines mark Blazhko candidate selection boundaries (see text).

ulation: direct light curve analysis and periodogram analysis, as 142
 follows. 143

3.1. Direct Light Curve Analysis

Given statistically correct period, amplitude and light curve 145 shape estimates, as well as data being consistent with reported 146 uncertainty estimates, the χ^2 per degree 147 of freedom gives a quantitative assessment of the "goodness of 148 fit", 149

$$\chi^2_{dof} = \frac{1}{N_{dof}} \sum \frac{(d_i - m_i)^2}{\sigma_i^2}. \quad (1)$$

Here, d_i are measured light curve data values at times t_i , and with 150 associated uncertainties σ_i , m_i are best-fit models at times t_i , and 151 N_{dof} is the number of degrees of freedom, essentially the number 152 of data points. In the absence of any light curve modulation, 153 the expected value of χ^2_{dof} is unity, with a standard deviation 154 of $\sqrt{2/N_{dof}}$. If $\chi^2_{dof} - 1$ is many times larger than $\sqrt{2/N_{dof}}$, 155 it is unlikely that data d_i were generated by the assumed (unchang- 156 ing) model m_i . Of course, χ^2_{dof} can also be large due to 157 underestimated measurement uncertainties σ_i , or to occasional 158 non-Gaussian measurement error (the so-called outliers). 159

Therefore, to search for signatures of the Blazhko effect, 160 manifested through statistically unlikely large values of χ^2_{dof} , we 161 computed χ^2_{dof} separately for LINEAR and ZTF data (see Figure 162 2). Using the two sets of χ^2_{dof} values, we algorithmically 163 pre-selected a sample of candidate Blazhko stars for further visual 164 analysis of their light curves. The visual analysis is needed to 165 confirm the expected Blazhko behavior in observed light curves, 166 as well as to identify cases of data problems, such as photometric 167 outliers. 168

Analysis of blazhko star metrics for RR Lyrae

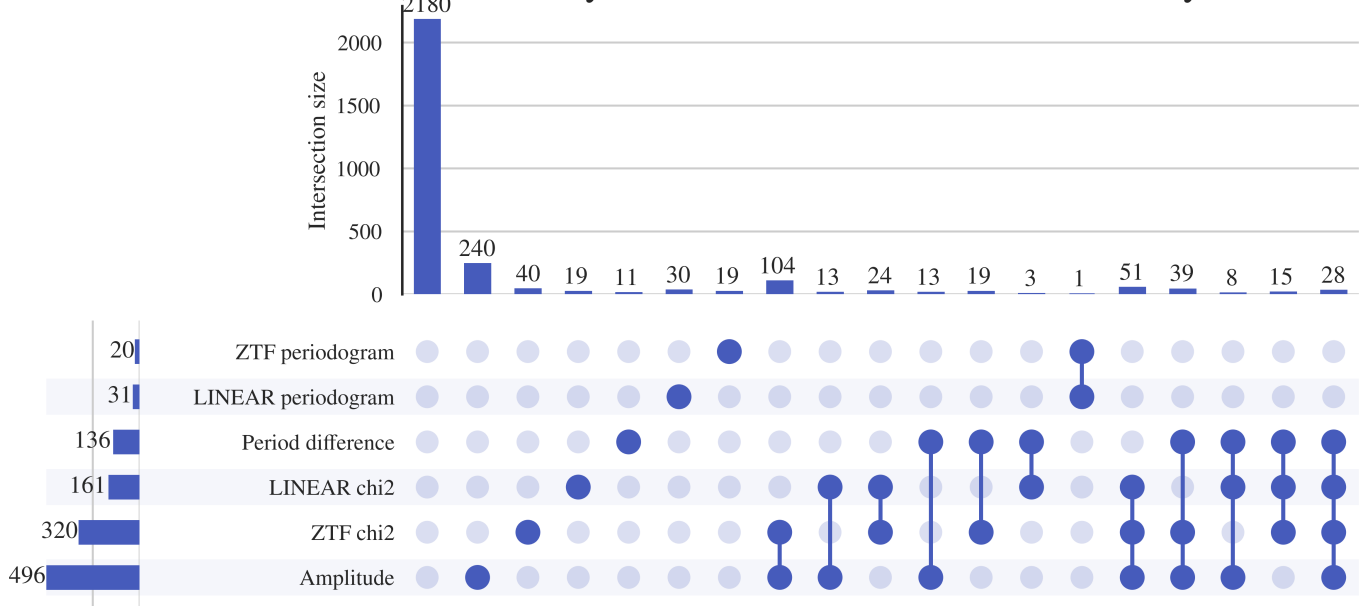


Fig. 3. The figure shows selection criteria and the resulting numbers of pre-selected Blazhko star candidates for each criterion and their combinations. The dots represent each case a star can occupy, where every solid dot is a specific criterion that is satisfied. Connections between solid dots represent stars which satisfy multiple criteria. Each dot combination has its own count, represented by the horizontal countplot. The vertical countplot shows the total number of stars that satisfy one criteria (union of all cases).

We used a simple scoring algorithm, optimized through trial and error, such that for LINEAR the range $1.8 < \chi^2_{dof} < 3.0$ was worth 2 points and $\chi^2_{dof} > 3.0$ worth 3 points, while for ZTF $2.0 < \chi^2_{dof} < 4.0$ and $\chi^2 > 4.0$ were the analogous limits. In addition, we also considered normalized period differences (dP) and amplitude differences (dA) and assigned: 2 points for $0.00002 < dP < 0.00005$ and 4 points for $dP > 0.00005$; 1 point for $0.05 < dA < 0.15$ and 2 points for $dA > 0.15$. A star could score a maximum of 12 points, and a minimum of 5 points was required for further visual analysis.

The sample pre-selected using this method includes 189 stars. For most selected stars, the χ^2_{dof} values were larger for the ZTF data because the ZTF photometric uncertainties are smaller than for the LINEAR data set. Fig. 3 summarizes the selection criteria and the resulting numbers of selected stars for each criterion and their combinations.

3.2. Periodogram Analysis

When light curve modulation is due to double-mode oscillation with two similar oscillation frequencies (periods), it is possible to recognize its signature in the periodogram computed as part of the Lomb-Scargle analysis. Depending on various details, such as data sampling and the exact values of periods, amplitudes, this method may be more efficient than direct light curve analysis (Skarka et al. 2020).

A sum of two *sine* functions with same amplitudes and with frequencies f_1 and f_2 can be rewritten using trigonometric equalities as

$$y(t) = 2 \cos(2\pi \frac{f_1 - f_2}{2} t) \sin(2\pi \frac{f_1 + f_2}{2} t). \quad (2)$$

We can define

$$f_o = \frac{f_1 + f_2}{2},$$

and

$$\Delta f = \left| \frac{f_1 - f_2}{2} \right|, \quad (4)$$

with $\Delta f \ll f_o$ when f_1 and f_2 are similar. The fact that Δf is much smaller than f_o means that the period of the *cos* term is much larger than the period of the basic oscillation (f_o). In other words, the *cos* term acts as a slow amplitude modulation of the basic oscillation. When the amplitudes of two *sine* functions are not equal, the results are more complicated but the basic conclusion about amplitude modulation remains. When the power spectrum of $y(t)$ is constructed, it will show 3 peaks: the main peak at f_o and two more peaks at frequencies $f_o \pm \Delta f$. We used this fact to construct an algorithm for automated searching for the evidence of amplitude modulation. Fig 4 compares the theoretical periodogram produced by interference beats with our algorithm's periodogram, signifying that local Blazhko peaks are present in real data.

After the strongest peak in the Lomb-Scargle periodogram is found at frequency f_o , we search for two equally distant local peaks at frequencies f_- and f_+ , with $f_- < f_o < f_+$. The side-band peaks can be highly asymmetric Alcock et al. (2003) and observed periodograms can sometimes be much more complex Szczygieł & Fabrycky (2007). We fold the periodogram through the main peak at f_o , multiply the two branches and then search for the strongest peaks in the resulting folded periodogram that is statistically more significant than the background noise. The background noise is computed as the scatter of the folded periodogram estimated from the interquartile range. We require a “signal-to-noise” ratio of at least 5, as well as the peak strength of at least 0.05. If such a peak is found, and it doesn't correspond to yearly alias, we select the star as a candidate Blazhko star and compute its Blazhko period as

$$P_{BL} = |f_{-,+} - f_o|^{-1},$$

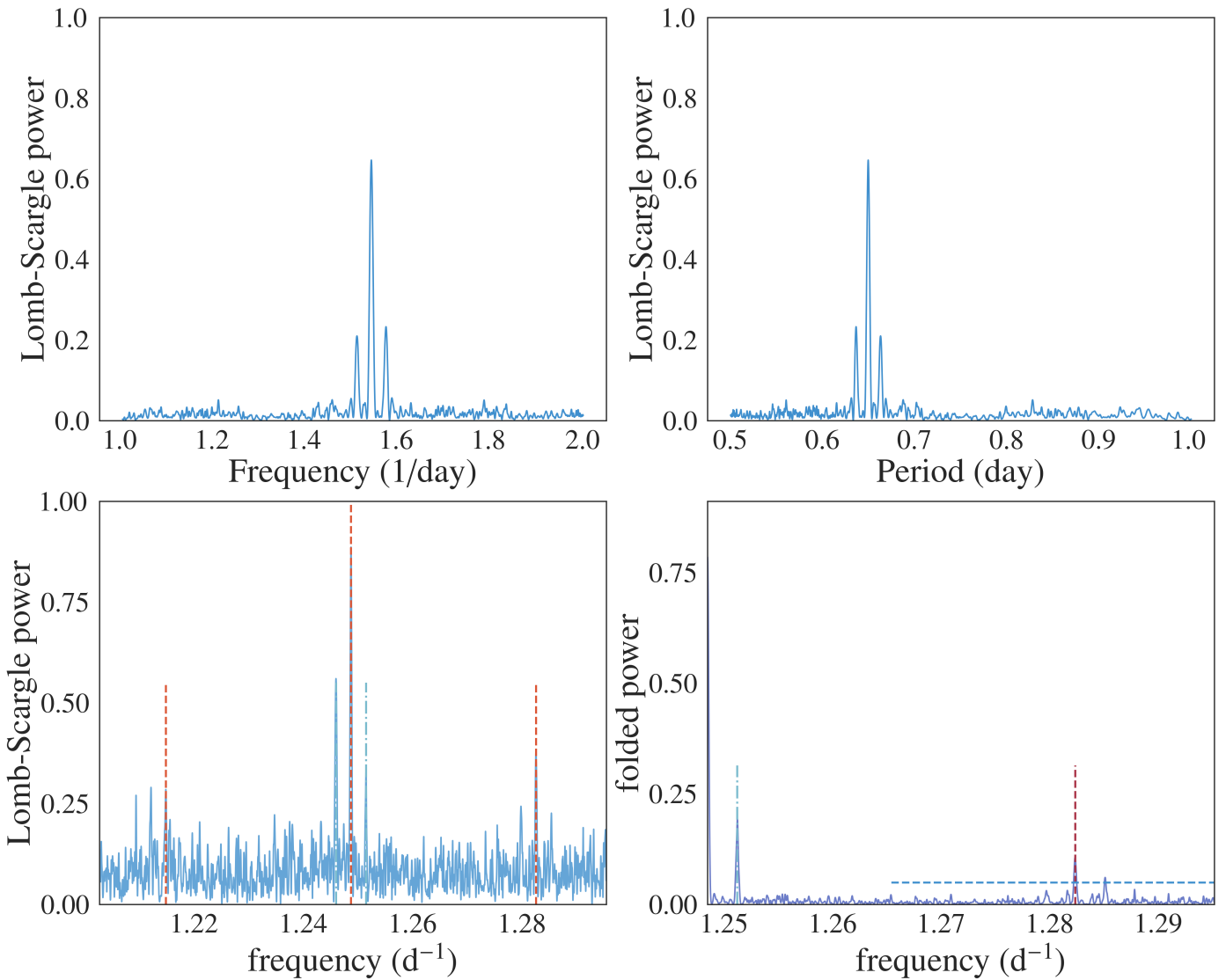


Fig. 4. The top two panels show a simulated periodogram for a sum of two *sine* functions with similar frequencies f_1 and f_2 – the central peak corresponds to their mean (see eqs. 3 and 4). The bottom left panel shows a periodogram for an observed LINEAR light curve, and the bottom right panel shows its folded version (around the main frequency $f_o = 1.585 \text{ d}^{-1}$). In the bottom left panel, the three vertical dashed lines show the three frequencies identified by the algorithm described in text, and the two dot-dashed lines mark yearly aliases around the main frequency f_o , at frequencies $f_o \pm 0.00274 \text{ d}^{-1}$. The two vertical lines in the bottom right panel have the same meaning, and the horizontal dashed line shows the noise level multiplied by 5.

where $f_{-,+}$ means the Blazhko sideband frequency with a higher amplitude is chosen.

The observed Blazhko periods range from 3 to 3,000 days, and Blazhko amplitudes range from 0.01 mag to about 0.3 mag (Szczygieł & Fabrycky 2007). In this work, we selected a smaller Blazhko range due to the limitations of our data: 30–325 days. With this additional constraint, we selected 51 candidate Blazhko stars, with one star already included in the sample of 189 stars described in preceding section. Fig ?? shows an example where two very prominent peaks were identified in the LINEAR periodogram.

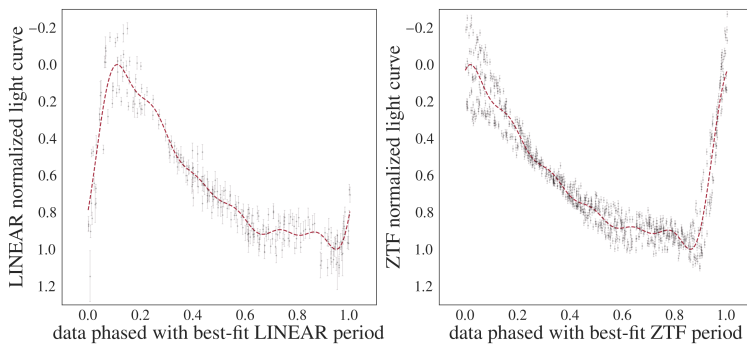
3.2.1. Visual Confirmation

The sample pre-selected for visual analysis includes 239 RR Lyrae stars (189 + 51, with one star selected twice), or 8.4% of the starting LINEAR-ZTF sample. Visual analysis includes

the following standard steps (e.g., Jurcsik et al. 2009; Prudil & Skarka 2017):

1. The shape of the phased light curves and scatter of data points around the best-fit model were examined for signatures of anomalous behavior indicative of the Blazhko effect. Fig. 5 shows an example of such behavior where the ZTF data and fit show multiple coherent data point sequences offset from the best-fit mean model.
2. Full light curves were inspected for their repeatability between observing seasons (Fig. 6). This step was sensitive to amplitude modulations with periods of the order a year or longer.
3. The phased light curves normalized to unit amplitude were inspected for their repeatability between observing seasons. This step was sensitive to phase modulations of a few percent or larger on time scales of the order a year or longer. Fig. 7 shows an example of a Blazhko star where season-to-

STAR 160 from 239



LINEAR period chi robust: 2.1, LINEAR mean period chi robust: 2.1
ZTF period chi robust: 4.4, ZTF mean period chi robust: 4.4
LINEAR period chi: 8.7, LINEAR mean period chi: 8.7
ZTF period chi: 34.2, ZTF mean period chi: 34.2
LINEAR period: 0.545073, ZTF period: 0.545074, Period difference: 0.0
Average LINEAR magnitude: 15.25
LINEAR amplitude: 0.75, ZTF amplitude: 0.82

Fig. 5. An illustration of visual analysis of phased light curves for the selected Blazhko candidates. The left panel shows LINEAR data and the right panel shows ZTF data (symbols with “error bars”) for star with LINEARid = 1212611. The dashed lines are best-fit models. The numbers listed on the right side were added to aid visual analysis. Note multiple coherent data point sequences offset from the best-fit mean model in the right panel.

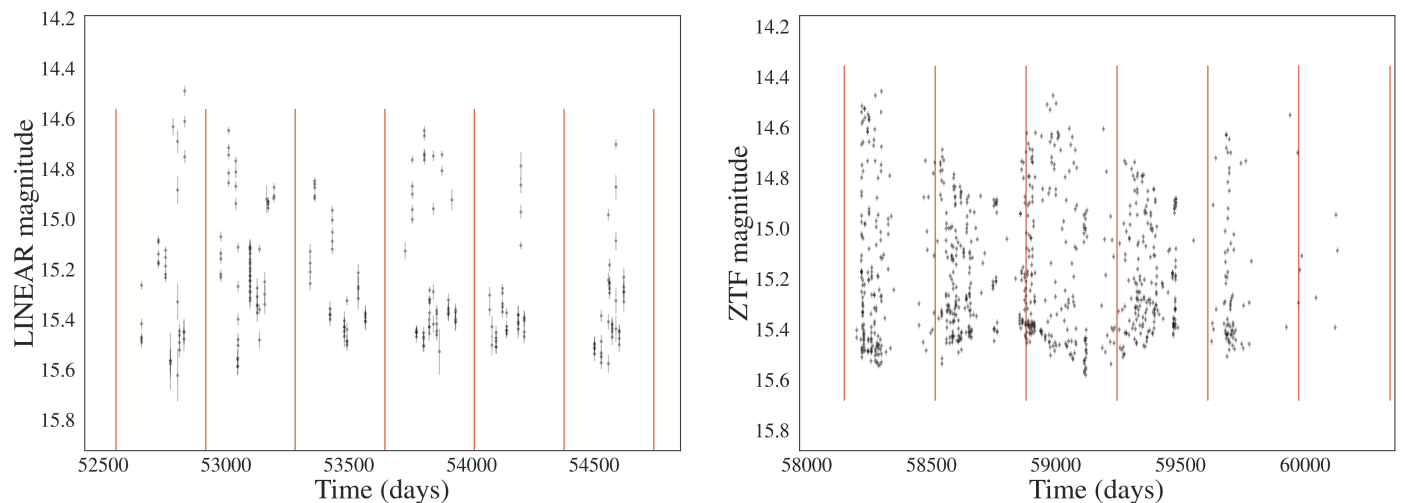


Fig. 6. An illustration of visual analysis of full light curves for the selected Blazhko candidates with emphasis on their repeatability between observing seasons, marked with vertical lines (left: LINEAR data; right: ZTF data). Data shown are for star with LINEARid = 1212611.

260 season phase (and amplitude) modulations are seen in both
261 the LINEAR data and (especially) the ZTF data.

262 After visually analyzing the starting sample of 239 Blazhko
263 candidates, we visually confirmed expected Blazhko behavior
264 for 136 stars (112 out of 189 and 24 out of 50). LINEAR IDs
265 and other characteristics for confirmed Blazhko stars are listed
266 in Table 1 (Appendix A). Statistical properties of the selected
267 sample of Blazhko stars are discussed in detail in the next sec-
268 tion.
269 STOPPED HERE

270 4. Results

271 UNFINISHED

272 Starting with a sample of 2857 field RR Lyrae stars with both
273 LINEAR and ZTF data, we found 136 stars exhibiting convinc-
274 ing Blazhko effect. In Appendix A, the reader can find all of the
275 Blazhko stars and some elementary data describing each star.

276 Another important note highlighting the difficulty of finding
277 Blazhko stars is that the absolute Blazhko frequency difference
278 from the main frequency is approximately $0.028 d^{-1}$. Also, the
279 average period difference between LINEAR and ZTF in Blazhko
280 stars was around 0.0001 days. These minimal differences require
281 precise observations over a long temporal baseline.

303

Finally, we have discovered that in some Blazhko stars, the
282 effect cannot be detected ten years later or beforehand. When
283 comparing LINEAR and ZTF data, some pairs have the effect
284 present in only one dataset and others in both. This finding could
285 mean that the Blazhko effect is not always present and gives us a
286 clue about its mechanism. However, the precision of data is also
287 a factor for consideration.

289 5. Discussion and Conclusions

290 UNFINISHED

291 The reported incidence rates for the Blazhko effect range
292 from 5% (Szczygieł & Fabrycky 2007) to 60% (Szabó et al.
293 2014). For a relatively small sample of 151 stars with Kepler
294 data, a claim has been made that essentially every RR Lyrae star
295 exhibits modulated light curve (Kovacs 2018). The difference in
296 Blazhko incidence rates for the two most extensive samples, ob-
297 tained by the OGLE-III survey for the Large Magellanic Cloud
298 (LMC, 20% out of 17,693 stars; Soszyński et al. 2009). More-
299 over, the Galactic bulge (30% out of 11,756 stars; Soszyński
300 et al. 2011) indicates a possible variation of the Blazhko inci-
301 dence rate with underlying stellar population properties. In this
302 work, 4.67% of the original RR Lyrae dataset are Blazhko stars.
303 Since our sample size is considerable, we conclude that the in-

Seasons for: 10030349

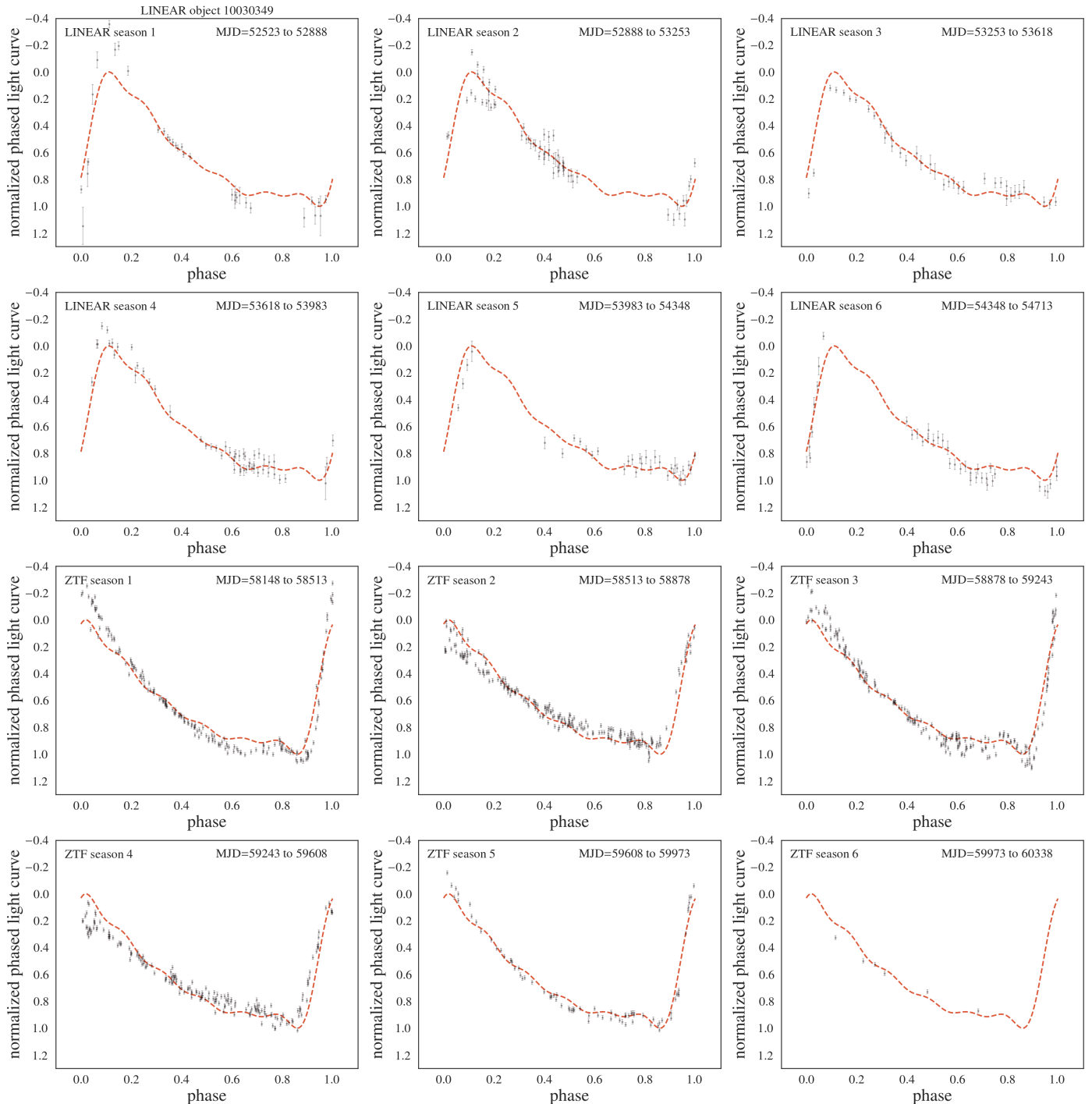


Fig. 7. The phased light curves normalized to unit amplitude are shown for single observing seasons and compared to the mean best-fit models (top six panels: LINEAR data; bottom six panels: ZTF data). Data shown are for star with LINEARid = 1212611. Season-to-season phase and amplitude modulations are seen in both the LINEAR and the ZTF data.

cidence rate of Blazhko stars in our work is representative and aligns with other works. We theorize that the difference in incidence rates occurs due to varying data precision, the temporal baseline length, and differences in visual or algorithmic analysis. We also conclude that our algorithm's success rate in finding 136 out of 239 potential Blazhko stars is 57%. This high number indicates that the algorithm is very successful and can be used and refined further for efficient Blazhko star selection.

319

For future research, we would like to explore the final finding and find a connection or a factor that might give rise to a mechanism that explains the Blazhko effect. The project is an excellent example of automatizing the search for Blazhko stars. It can further be improved by training a neural network to replace visual analysis, and our current algorithms can be improved with other models. This work can provide a base for finding more Blazhko stars for the future Vera Rubin observatory. The Legacy Survey

312
313
314
315
316
317

of Space and Time (LSST; Ivezić et al. 2019) will be an excellent survey for studying Blazhko effect (Hernitschek & Stassun 2022) because it will have both a long temporal baseline (10 years) and a large number of observations per object (nominally 825; LSST Science Requirements Document⁴).

Claim from the abstract: With time-resolved photometry expected from LSST, a similar analysis will be performed for RR Lyrae stars in the southern sky and we anticipate a higher fraction of discovered Blazhko stars due to better sampling and superior photometric quality. Support with this quote:

the incidence rate of the Blazhko effect increases with sensitivity to small-amplitude modulation, and thus with photometric data quality (Jurcsik et al. 2009).

We confirm that the light curve modulation can be unstable, as discussed by Jurcsik et al. (2009)

(Skarka et al. 2020) classify Blazhko stars in 6 classes using the morphology of their amplitude modulation (though we note that the most dominant class includes 90% of the sample). They find bimodal distribution of Blazhko periods, with two components centered on 48 d and 186 d.

LINEAR and ZTF data used here do not have as many data points as OGLE-III used by them (comment earlier, in Introduction? also Kepler is great, (Benkő et al. 2010)). Emphasize 22 years from the start of LINEAR to the end of ZTF light curves. Also, ZTF goes deeper.

From Jurcsik et al. (2009): A sample of 30 RRab stars was extensively observed, and light-curve modulation was detected in 14 cases. The 47 per cent occurrence rate of the modulation is much larger than any previous estimate.

Acknowledgements. We thank Mathew Graham for providing *ztfquery* code example to us. Ž.I. acknowledges funding by the Fulbright Foundation and thanks the Ruđer Bošković Institute (Zagreb, Croatia) for hospitality. Based on observations obtained with the Samuel Oschin Telescope 48-inch and the 60-inch Telescope at the Palomar Observatory as part of the Zwicky Transient Facility project. ZTF is supported by the National Science Foundation under Grants No. AST-1440341 and AST-2034437 and a collaboration including current partners Caltech, IPAC, the Weizmann Institute of Science, the Oskar Klein Center at Stockholm University, the University of Maryland, Deutsches Elektronen-Synchrotron and Humboldt University, the TANGO Consortium of Taiwan, the University of Wisconsin at Milwaukee, Trinity College Dublin, Lawrence Livermore National Laboratories, IN2P3, University of Warwick, Ruhr University Bochum, Northwestern University and former partners the University of Washington, Los Alamos National Laboratories, and Lawrence Berkeley National Laboratories. Operations are conducted by COO, IPAC, and UW. The LINEAR program is funded by the National Aeronautics and Space Administration at MIT Lincoln Laboratory under Air Force Contract FA8721-05-C-0002. Opinions, interpretations, conclusions and recommendations are those of the authors and are not necessarily endorsed by the United States Government.

References

Alcock, C., Alves, D. R., Becker, A., et al. 2003, ApJ, 598, 597	369
Astropy Collaboration, Price-Whelan, A. M., Sipőcz, B. M., et al. 2018, AJ, 156, 123	370
Bellm, E. C., Kulkarni, S. R., Graham, M. J., et al. 2019, PASP, 131, 018002	371
Benkő, J. M., Kolenberg, K., Szabó, R., et al. 2010, MNRAS, 409, 1585	372
Blažko, S. 1907, Astronomische Nachrichten, 175, 325	373
Catelan, M. 2009, Ap&SS, 320, 261	374
Hernitschek, N. & Stassun, K. G. 2022, ApJS, 258, 4	375
Ivezić, Ž., Kahn, S. M., Tyson, J. A., et al. 2019, ApJ, 873, 111	376
Jurcsik, J., Sódor, Á., Szeidl, B., et al. 2009, MNRAS, 400, 1006	377
Kolenberg, K. 2008, in Journal of Physics Conference Series, Vol. 118, Journal of Physics Conference Series (IOP), 012060	378
Kovács, G. 2009, in American Institute of Physics Conference Series, Vol. 1170, Stellar Pulsation: Challenges for Theory and Observation, ed. J. A. Guzik & P. A. Bradley, 261–272	379
Kovács, G. 2016, Communications of the Konkoly Observatory Hungary, 105, 61	380
Kovács, G. 2018, A&A, 614, L4	381
Mizerski, T. 2003, Acta Astron., 53, 307	382
Palaversa, L., Ivezić, Ž., Eyer, L., et al. 2013, AJ, 146, 101	383
Prudil, Z. & Skarka, M. 2017, MNRAS, 466, 2602	384
Sesar, B., Ivezić, Ž., Grammer, S. H., et al. 2010, ApJ, 708, 717	385
Sesar, B., Ivezić, Ž., Stuart, J. S., et al. 2013, AJ, 146, 21	386
Sesar, B., Stuart, J. S., Ivezić, Ž., et al. 2011, AJ, 142, 190	387
Skarka, M., Prudil, Z., & Jurcsik, J. 2020, MNRAS, 494, 1237	388
Smith, H. A. 1995, Cambridge Astrophysics Series, 27	389
Soszyński, I., Dziembowski, W. A., Udalski, A., et al. 2011, Acta Astron., 61, 1	390
Soszyński, I., Udalski, A., Szymański, M. K., et al. 2010, Acta Astron., 60, 165	391
Soszyński, I., Udalski, A., Szymański, M. K., et al. 2009, Acta Astron., 59, 1	392
Szabó, R. 2014, in IAU Symposium, Vol. 301, Precision Asteroseismology, ed. J. A. Guzik, W. J. Chaplin, G. Handler, & A. Pigulski, 241–248	393
Szabó, R., Benkő, J. M., Paparó, M., et al. 2014, A&A, 570, A100	394
Szczygiel, D. M. & Fabrycky, D. C. 2007, MNRAS, 377, 1263	395
Vanderplas, J. 2015, gatspy: General tools for Astronomical Time Series in Python	396
VanderPlas, J., Connolly, A. J., Ivezić, Z., & Gray, A. 2012, in Proceedings of Conference on Intelligent Data Understanding (CIDU, 47–54	397

366

367

⁴ Available as ls.st/srd

406 **Appendix A: Full table of results**

407 Here we present all the confirmed Blazhko stars with their LINEAR IDs, equatorial coordinates, and calculated periods and χ^2 val-

LINEAR ID	Plinear	Pztf	N_L	N_Z	L_chi2r	Z_chi2r	L_chi2	Z_chi2	Lampl	Zampl	
29848	0.557020	0.557040	301	43	1.4	3.5	3.0	12.6	0.56	0.93	
50402	0.643303	0.643294	284	586	0.7	1.1	0.6	1.8	0.48	0.69	
62892	0.530776	0.530785	276	771	0.9	3.2	1.1	19.8	0.62	0.64	
91437	0.674733	0.674737	177	564	1.3	2.0	2.8	5.6	0.87	1.21	
95250	0.313870	0.313876	222	916	0.8	1.4	0.8	3.0	0.48	0.46	
104455	0.997195	0.997587	119	44	1.6	17.6	3.4	184.1	4141.12	42446.41	
108513	0.473809	1.000362	282	42	1.4	10.9	4.0	161.1	0.86	26072.93	
136668	0.532923	0.532929	310	918	1.1	2.3	1.6	17.0	0.82	0.78	
141414	0.335690	0.335669	278	919	0.8	1.5	0.6	2.6	0.41	0.37	
142794	0.470787	0.470802	270	63	1.0	2.3	1.8	11.9	0.72	0.72	
158779	0.609207	0.609189	293	616	1.6	3.9	3.7	34.2	0.47	0.68	
162255	0.512747	0.512744	266	1119	1.6	1.6	5.7	6.2	0.96	1.31	
163933	0.339629	0.679246	306	53	0.9	0.9	1.0	1.5	0.45	0.35	
172382	0.458309	0.458308	227	1461	1.1	2.4	1.5	10.2	1.16	1.10	
174389	0.334036	0.334040	270	786	1.4	1.4	4.5	2.2	0.27	0.33	
186102	0.647419	0.647425	188	574	0.7	1.3	0.6	2.6	0.89	1.11	
215632	0.572162	0.572163	286	441	1.0	1.4	0.9	3.4	0.75	0.99	
258499	0.401505	0.401504	275	537	1.5	1.6	2.7	2.9	0.34	0.36	
263541	0.558218	0.558221	270	503	2.9	6.6	15.8	110.4	0.64	0.82	
303860	0.499321	0.492164	280	639	5.0	4.3	36.3	83.8	86.75	1.08	
309626	0.595841	0.997215	215	40	2.9	16.5	21.0	445.4	0.68	868885.53	
355767	0.499298	0.521363	180	114	3.4	1.8	9.5	4.5	4622.25	1.12	
393084	0.530027	0.530033	493	372	1.1	3.2	1.6	19.2	0.96	1.31	
418785	0.700122	0.700120	263	50	0.8	0.9	1.4	1.3	0.56	0.44	
420327	0.535225	0.535220	144	656	0.8	1.4	1.1	2.8	0.53	0.74	
437483	0.699234	0.699235	316	666	0.7	1.0	0.5	1.7	0.37	0.35	
439441	0.709248	0.709247	349	443	1.3	1.4	2.1	2.4	0.36	0.50	
514883	0.557723	0.557737	289	555	1.7	5.5	5.3	53.7	0.55	0.72	
516954	0.297570	0.297569	243	1164	2.3	1.3	5.6	2.7	0.52	0.60	
523832	0.372376	0.372384	251	42	1.2	1.1	1.8	0.8	0.42	0.59	
558961	0.600532	0.600547	213	61	2.2	1.7	11.9	2.0	0.55	0.55	
608497	0.485636	0.748671	556	37	2.5	10.5	20.4	504.9	0.86	19.10	
658512	0.969050	2.708902	404	42	1.5	5.4	2.4	25.0	0.31	0.67	
664583	0.602994	0.603021	449	613	1.1	2.5	1.8	11.1	0.56	0.53	
670864	0.600802	0.395810	336	42	0.9	10.6	1.2	115.1	0.52	23.53	
717668	0.426744	0.426758	302	428	1.2	1.7	1.6	3.9	0.32	0.32	
734545	0.289482	0.702579	305	41	1.7	5.4	3.3	28.6	0.29	0.44	
737951	0.357023	0.357023	273	871	2.2	6.7	6.0	42.4	0.43	0.34	
771232	0.540930	0.540941	301	889	1.0	1.6	1.1	4.7	0.93	0.89	
798477	0.651627	0.651611	294	139	1.2	3.5	2.0	17.8	0.61	0.78	
803829	0.595281	0.595286	270	561	2.3	2.6	8.7	9.9	0.91	1.34	
810169	0.465185	0.465212	289	743	2.1	2.8	6.0	15.1	0.77	0.75	
813450	0.589387	0.589389	221	431	1.3	1.0	2.0	2.3	0.70	0.93	
836895	0.473399	0.473398	194	612	1.3	2.8	3.0	11.1	1.09	1.49	
843294	0.374216	0.374214	290	358	1.4	1.7	3.3	5.1	0.36	0.36	
851716	1.908191	0.388356	100	147	1.2	5.3	1.3	39.7	0.64	0.38	
856862	0.625858	1.251798	294	26	1.0	1.2	1.1	1.6	0.45	0.60	
869112	0.635690	1.753223	322	32	0.9	2.1	1.0	4.4	0.34	0.54	
872620	0.549247	0.549248	282	272	1.0	1.5	1.1	2.8	0.85	0.63	
880568	0.628261	1.157215	200	30	2.5	1.6	19.6	19.2	0.73	0.74	
880588	0.600138	0.600134	295	442	1.2	2.4	3.2	23.4	0.91	0.84	
883073	0.725513	2.661727	302	32	1.0	2.9	1.0	9.5	0.43	0.61	
895953	0.658156	0.658154	297	408	0.7	1.5	0.5	3.4	0.46	0.50	
899832	0.589463	12.401002	285	6	2.1	0.2	9.3	0.0	0.61	255.00	
924301	0.507503	0.507440	418	189	1.9	9.3	13.8	162.9	0.87	0.79	
966279	0.517279	0.517270	330	607	1.5	2.7	6.1	21.0	0.92	0.82	
967924	0.643331	0.643319	227	569	0.9	1.4	0.7	3.0	0.92	1.27	
968962	0.579336	0.579334	235	711	1.0	1.4	1.1	3.4	0.84	0.80	
969277	1.003276	0.691657	220	676	2.8	1.2	13.0	2.5	0.55	0.75	
970326	0.592233	0.592231	275	552	1.1	2.1	1.9	7.7	0.51	0.75	
976746	0.620673	0.620663	236	91	1.6	1.4	3.9	2.3	0.45	0.40	
Article number, page 10 of 10	989567	0.632456	283	69	1.1	2.3	1.4	4.4	0.25	0.80	
	991055	0.347282	0.997648	131	104	1.3	12.2	2.7	130.4	0.43	16.81
	993105	0.794678	0.794668	205	115	0.9	1.0	0.9	1.0	0.34	0.23
	999528	0.658401	0.658407	564	213	1.2	2.7	1.8	21.7	0.57	0.92
	1004849	0.458463	0.458467	607	193	1.3	2.6	6.5	14.7	1.14	1.60
	1005497	0.653607	0.653605	607	192	1.1	2.1	2.1	12.4	0.60	0.83
	1012000	0.584572	0.584528	220	106	1.2	1.4	1.4	22.0	0.72	0.48